An Observational Study of the Dependence of Ocean Surface Filaments on Wind Speed

Rick Danielson, Hui Shen, Jing Tao, Will Perrie,
Fisheries and Oceans Canada, Bedford Institute of Oceanography

- What synthetic aperture radar (SAR) filaments might tell us about the search for North Atlantic Right Whale (NARW) prey (i.e., zooplankton aggregations)
- Specific measurements of filaments and wind speed in the Gulf of St. Lawrence
- Correlation and wind adjustment
- Summary of modeling considerations

Acknowledgements

Funding was provided by the Competitive Science Research Fund (CSRF) and Species at Risk (also denoted SAR) Program of Fisheries and Oceans Canada. We thank the North Atlantic Right Whale Consortium and Team Whale of Fisheries and Oceans Canada for their efforts in collecting and quality controlling the Gulf of St. Lawrence whale sightings. Radarsat data were produced by MacDonald, Dettwiler and Associates Ltd. and obtained from the Earth Observation Data Management System of Natural Resources Canada. The ERA5 data were obtained from the Copernicus Climate Change Service (C3S) Climate Data Store. We thank M. Rizzo and G. Szekely for providing the distance correlation R package (energy). Please see https://arxiv.org/abs/2302.01533 for more details or reach out by email to rick.danielson@dfo-mpo.gc.ca.

What can SAR filaments tell us about zooplankton?

- An estimated 340 North Atlantic right whales are alive today (and in decline?)
- Perhaps 40% (~40 females) now forage in the Gulf of St. Lawrence during May-Nov
- **Right whale presence is among the best indications of zooplankton aggregation**
- Sorochan et al. (2021) point to prey aggregation at depth, and transient aggregation near the surface, in regions delimited by tidal mixing and freshwater pulses, and in convergent circulations in the upper mixed layer (their Fig. 5a)
- Unlike Lyapunov exponents (Maps et al. 2015), SAR filaments depend on more than ocean current deformation…

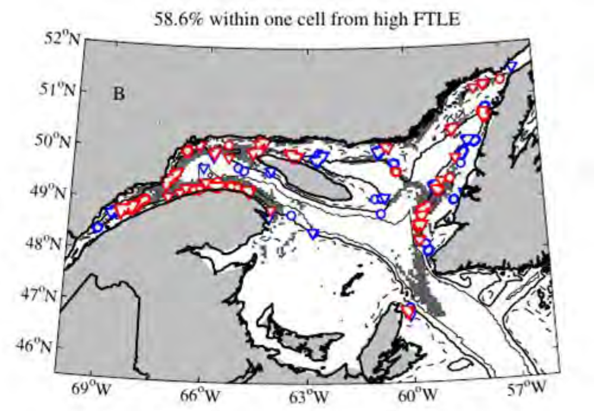

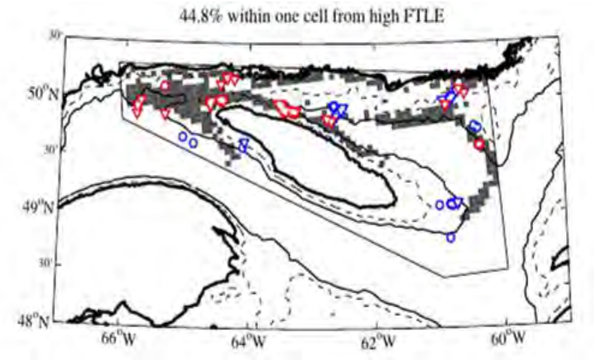

Maps, F., S. Plourde, I. H. McQuinn, S. St. Onge-Drouin, D. Lavoie, J. Chassé, and V. Lesage, 2015: **Linking acoustics and finite-time Lyapunov exponents reveals areas and mechanisms of krill aggregation within the Gulf of St. Lawrence, eastern Canada.** Limnol. Oceanogr., 60, 1965–1975, doi:10.1002/lno.10145.

Sorochan, K. A., S. Plourde, M. F. Baumgartner, and C. L. Johnson, 2021: **Availability, supply, and aggregation of prey (Calanus spp.) in foraging areas of the North Atlantic right whale (*Eubalaena glacialis*).** ICES J. Mar. Sci., 78, doi:10.1093/icesjms/fsab200.

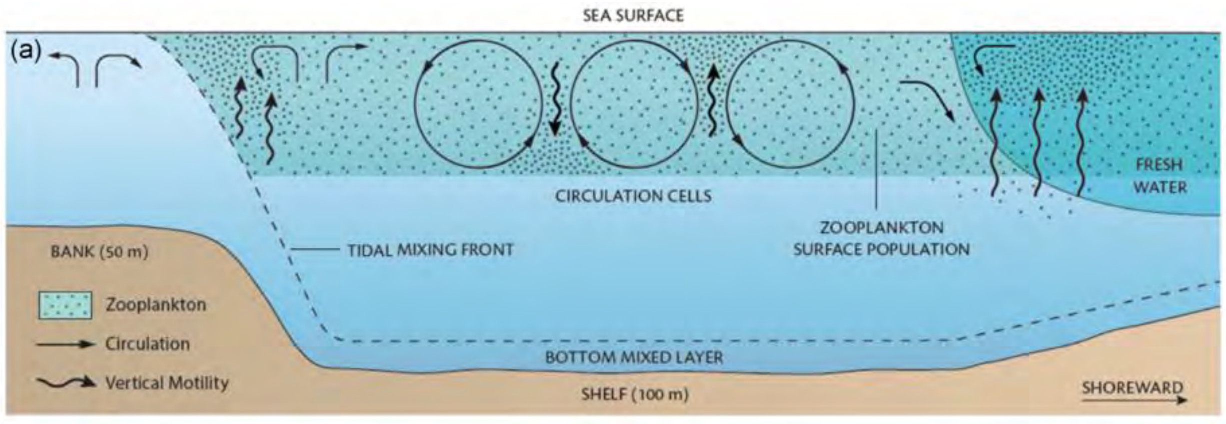

What can SAR filaments tell us about zooplankton?

- Munk et al. (2000) highlight wind speed dependence, where "**under light winds favourable to visualization, linear surface features** [i.e., filaments] **with high surfactant density and low surface roughness are of common occurrence**."
- SAR also offers a view of ocean currents modulating waves and wave breaking, and in turn, surface roughness at wind speeds up to 10 ms^{-1} (Rascle et al. 2017). A SAR contrast model and its observational equivalent are given by Kudryavtsev et al. (2012) as

Model $$\frac{\tilde{q}}{q_0} = -c_q \ln\left(\frac{u_* k_b}{g^{1/2} K^{1/2}}\right) \frac{g}{u_*^2 k_b} \omega_b^{-1} \nabla \cdot \boldsymbol{u}$$

Observational Equivalent $$\frac{\sigma_\circ - \overline{\sigma_\circ}}{\overline{\sigma_\circ}}$$

- But like any "primitive equation" model, **this does not specify measurements themselves,** including SAR backscatter (σ_o), friction velocity (u_*), and ocean current convergence ($-\nabla \cdot \boldsymbol{u}$)
- Our study begins by defining the measurements of interest, and approaches the question of dependence by asking **how specific measurements may be associated** (Cochran 1972)

Munk W., L. Armi, K. Fischer, and F. Zachariasen (2000) Spirals on the sea, *Proc. R. Soc. Lond. A.*, 456, 1217–1280.

Rascle, N., Molemaker, J., Marié, L., Nouguier, F., Chapron, B., Lund, B., Mouche, A., 2017. Intense deformation field at oceanic front inferred from directional sea surface roughness observations, Geophys. Res. Lett. 44, 5599-5608, doi:10.1002/2017GL073473.

Kudryavtsev, V., A. Myasoedov, B. Chapron, J. A. Johannessen, and F. Collard (2012), Imaging mesoscale upper ocean dynamics using synthetic aperture radar and optical data, J. Geophys. Res., 117, C04029, doi:10.1029/2011JC007492.

Cochran, W. G., 1972. Observational studies, Statistical Papers in Honor of George W. Snedecor, T. A. Bancroft, Ed., Iowa State University Press, pp. 77{90, 2015 reprint doi:10.1353/obs.2015.0010.

Specific measurements in the Gulf of St. Lawrence

Radarsat-2
SAR contrast

$$\frac{\sigma_o - \overline{\sigma_o}}{\overline{\sigma_o}}$$

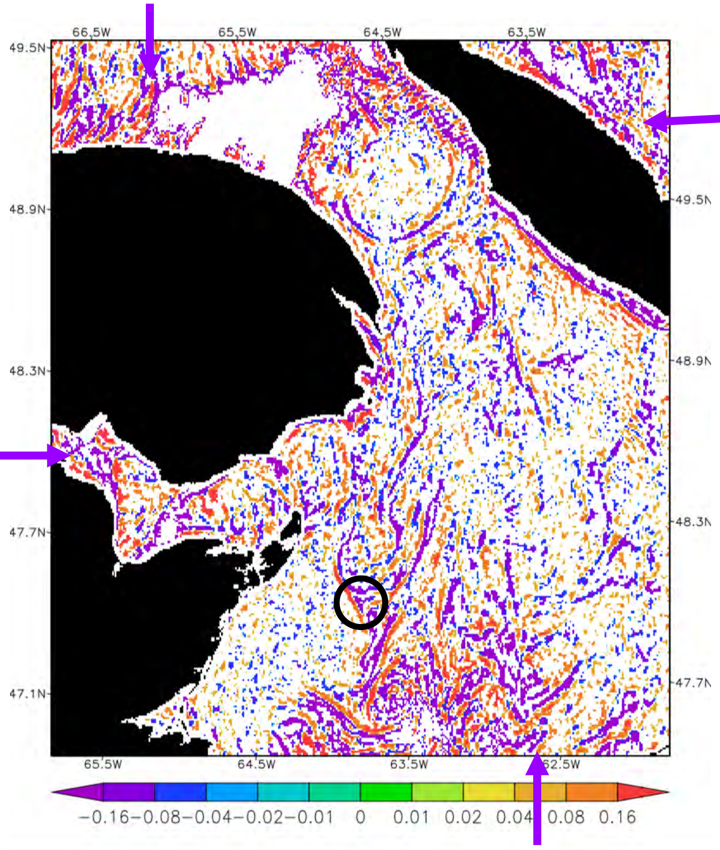

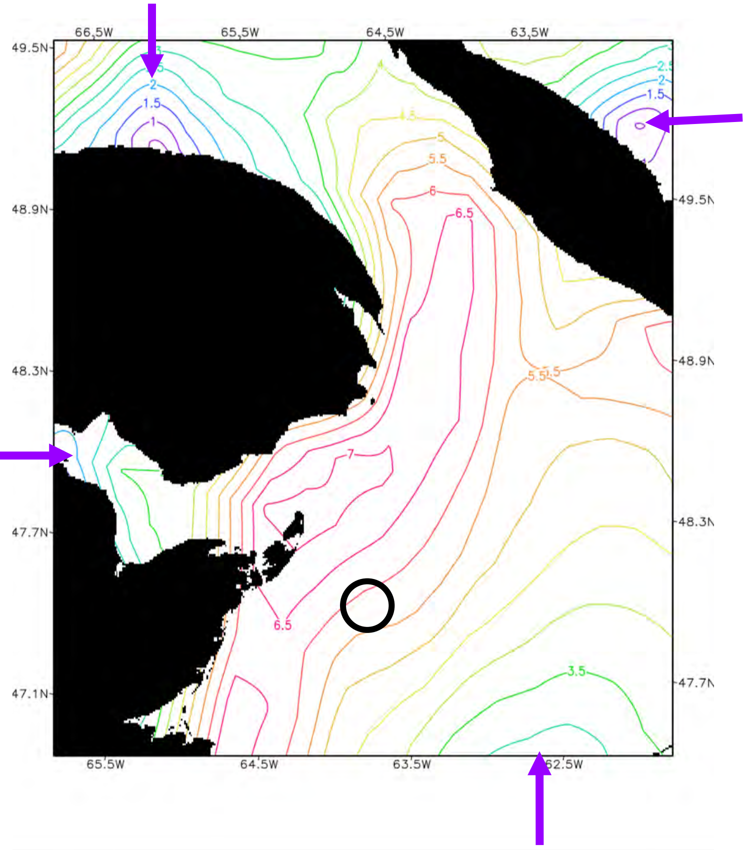

ERA5 weak
wind speed (ms^{-1})

○

21 right whales
sighted on
July 26, 2019
(SAR at 21:59)

○ A search for right whale prey is more interesting in the presence of whales, but as expected, Radarsat-2 SAR contrast is relatively strong where ERA5 wind speed is weak (we mask very small σ_o and avoid wind speed > 10 ms^{-1}). **Because wind speed varies across a SAR scene and between scenes, can we quantify (and partially remove) the dependence of Radarsat-2 contrast on ERA5 wind speed?**

Specific measurements in the Gulf of St. Lawrence

A total of **941** Radarsat-2 SAR scenes from April to December 2008-2020 overlap with the dashed line

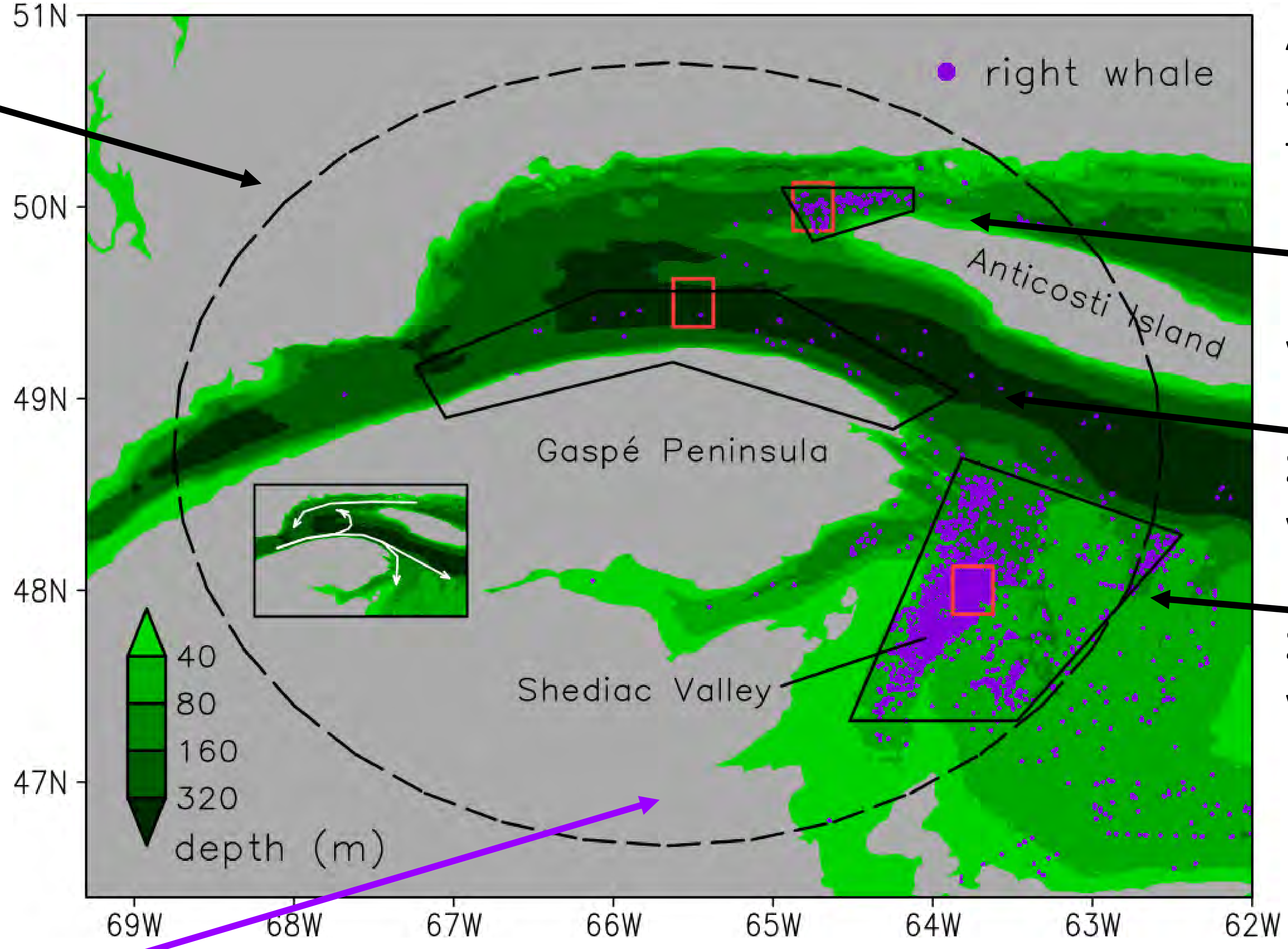

A subset of **324** SAR scenes from mid-May to mid-August:

177 scenes overlap with **Anticosti** domain

241 scenes overlap with **Gaspé** domain

237 scenes overlap with **Shediac** domain

Most right whale sightings between 2015-2020 are in the Shediac Valley

ERA5 wind speed collocations

Specific measurements in the Gulf of St. Lawrence

Smooth σ_O to 100, 200, 400, 800, 1600, 3200, 6400, and 12800-m resolution

Average contrast of the same sign (σ_O at 800m and $\overline{\sigma_O}$ at 1600/3200/6400m)

Weight contrast by ERA5 wind speed to reduce SAR-wind association

Group adjacent contrasts (small groups < O[10km] are set to zero)

Average contrast magnitude in *fixed* domains (Anticosti, Gaspé, and Shediac)

Processing Radarsat-2 SAR contrast

$$\frac{\sigma_\circ - \overline{\sigma_\circ}}{\overline{\sigma_\circ}}$$

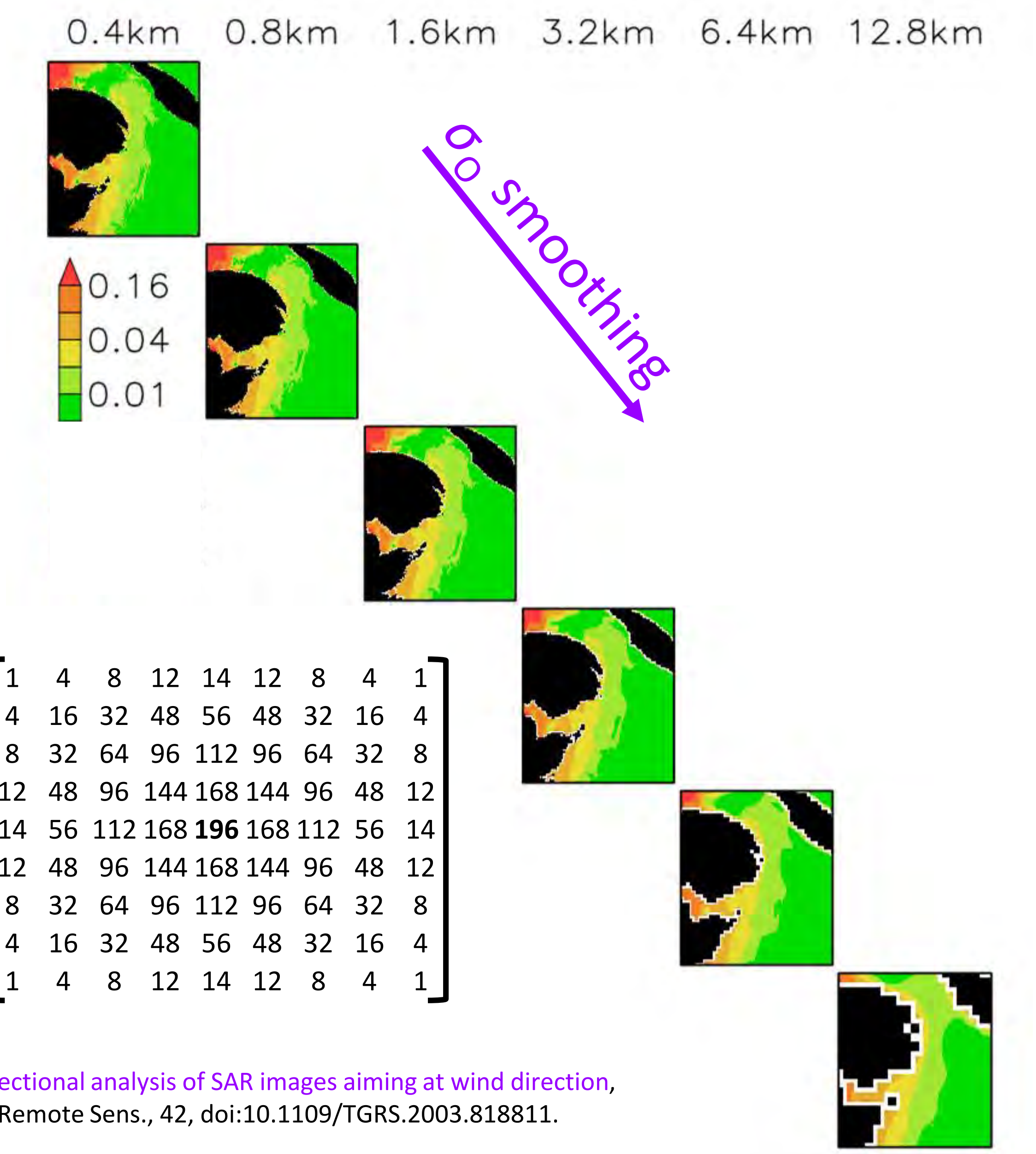

$$R^2 = \frac{1}{4096}\begin{bmatrix} 1 & 4 & 8 & 12 & 14 & 12 & 8 & 4 & 1 \\ 4 & 16 & 32 & 48 & 56 & 48 & 32 & 16 & 4 \\ 8 & 32 & 64 & 96 & 112 & 96 & 64 & 32 & 8 \\ 12 & 48 & 96 & 144 & 168 & 144 & 96 & 48 & 12 \\ 14 & 56 & 112 & 168 & \mathbf{196} & 168 & 112 & 56 & 14 \\ 12 & 48 & 96 & 144 & 168 & 144 & 96 & 48 & 12 \\ 8 & 32 & 64 & 96 & 112 & 96 & 64 & 32 & 8 \\ 4 & 16 & 32 & 48 & 56 & 48 & 32 & 16 & 4 \\ 1 & 4 & 8 & 12 & 14 & 12 & 8 & 4 & 1 \end{bmatrix}$$

Koch, W., 2004: Directional analysis of SAR images aiming at wind direction, IEEE Trans. Geosci. Remote Sens., 42, doi:10.1109/TGRS.2003.818811.

Specific measurements in the Gulf of St. Lawrence

Smooth σ_O to 100, 200, 400, 800, 1600, 3200, 6400, and 12800-m resolution

Average contrast of the same sign (σ_O at 800m and $\overline{\sigma_O}$ at 1600/3200/6400m)

Weight contrast by ERA5 wind speed to reduce SAR-wind association

Group adjacent contrasts (small groups < O[10km] are set to zero)

Average contrast magnitude in *fixed* domains (Anticosti, Gaspé, and Shediac)

Processing Radarsat-2 SAR contrast

$$\frac{\sigma_o - \overline{\sigma_o}}{\overline{\sigma_o}}$$

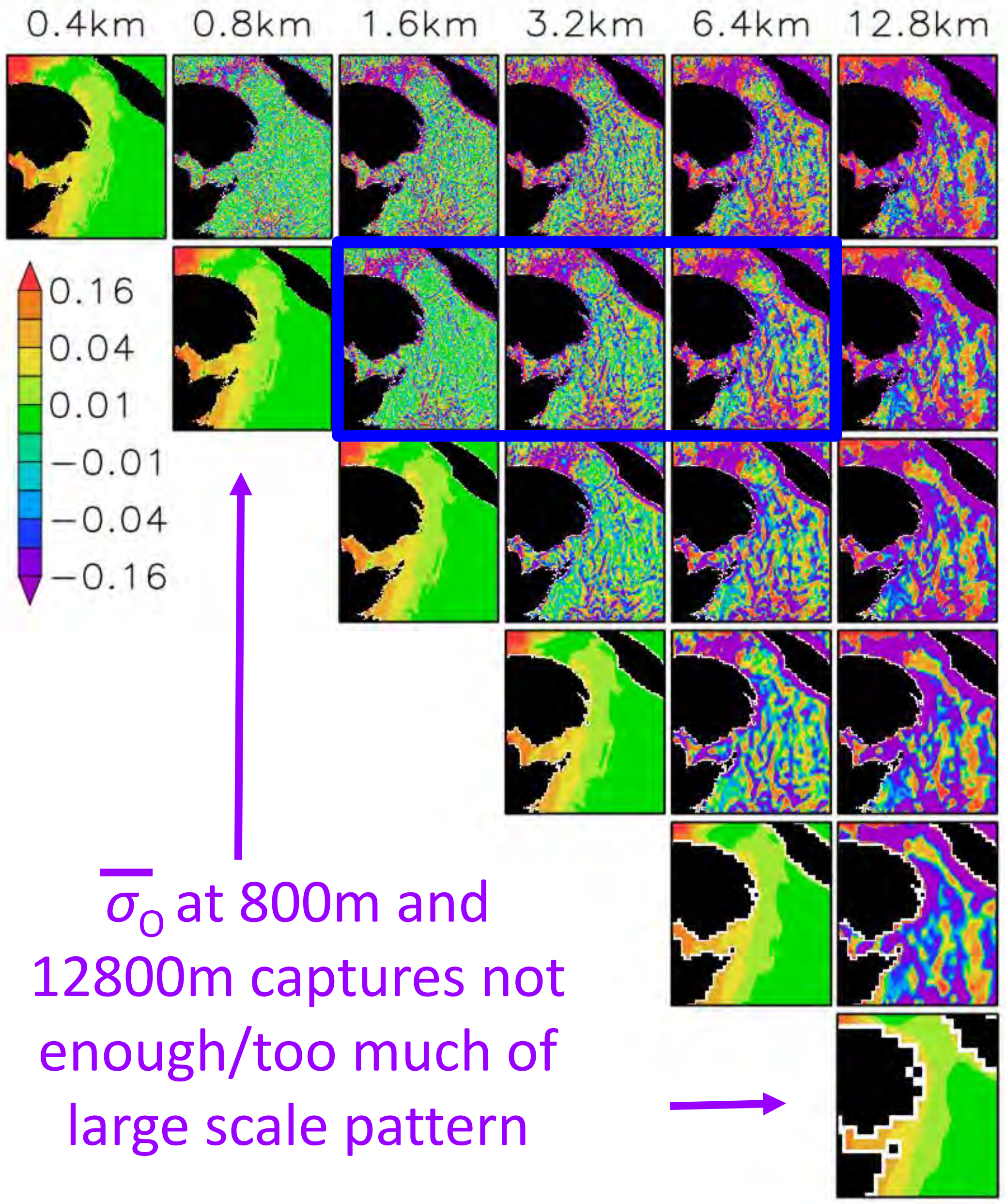

$\overline{\sigma_O}$ at 800m and 12800m captures not enough/too much of large scale pattern

Specific measurements in the Gulf of St. Lawrence

Smooth σ_O to 100, 200, 400, 800, 1600, 3200, 6400, and 12800-m resolution

Average contrast of the same sign (σ_O at 800m and $\overline{\sigma_O}$ at 1600/3200/6400m)

Weight contrast by ERA5 wind speed to reduce SAR-wind association

Group adjacent contrasts (small groups < O[10km] are set to zero)

Average contrast magnitude in *fixed* domains (Anticosti, Gaspé, and Shediac)

Unweighted

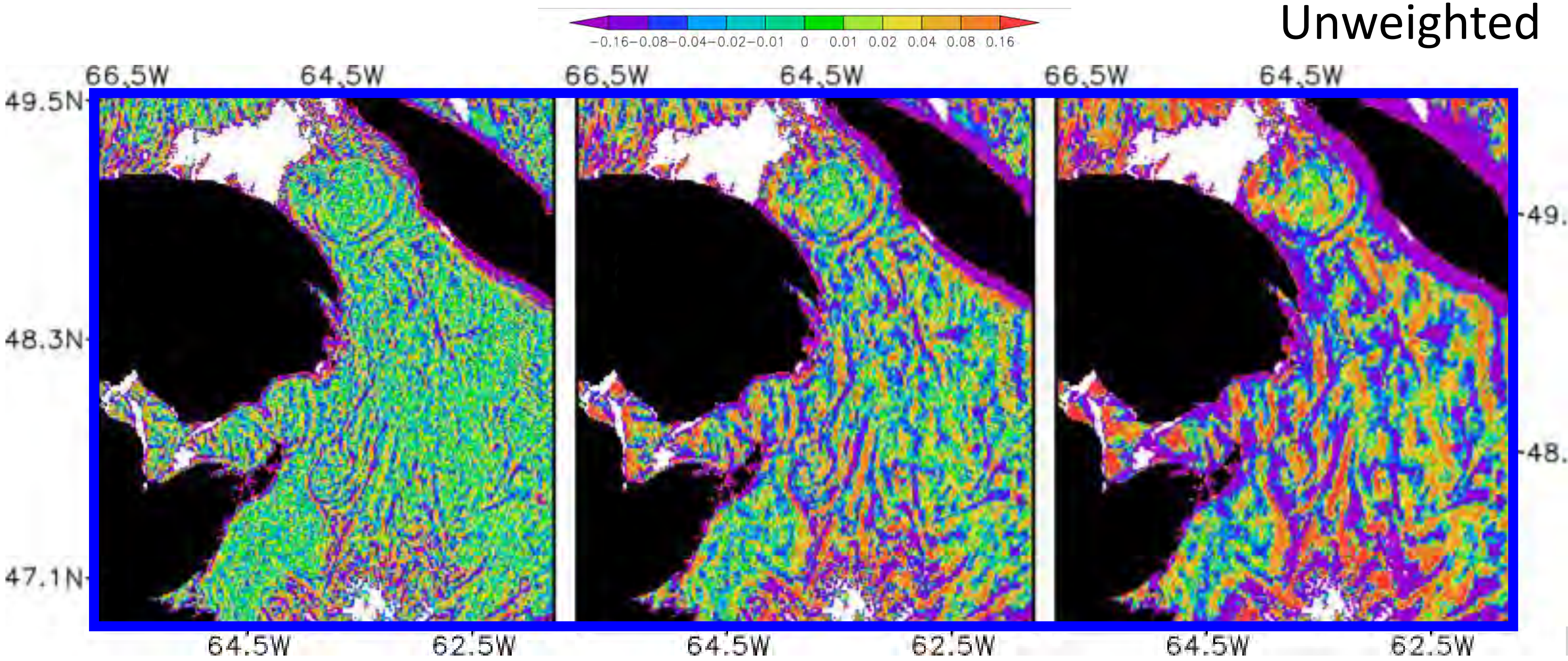

Agreement in sign of contrast helps to isolate filamentary SAR pattern

Specific measurements in the Gulf of St. Lawrence

Smooth σ_O to 100, 200, 400, 800, 1600, 3200, 6400, and 12800-m resolution

Average contrast of the same sign (σ_O at 800m and $\overline{\sigma_O}$ at 1600/3200/6400m)

Weight contrast by ERA5 wind speed to reduce SAR-wind association

Group adjacent contrasts (small groups < O[10km] are set to zero)

Average contrast magnitude in *fixed* domains (Anticosti, Gaspé, and Shediac)

Unweighted

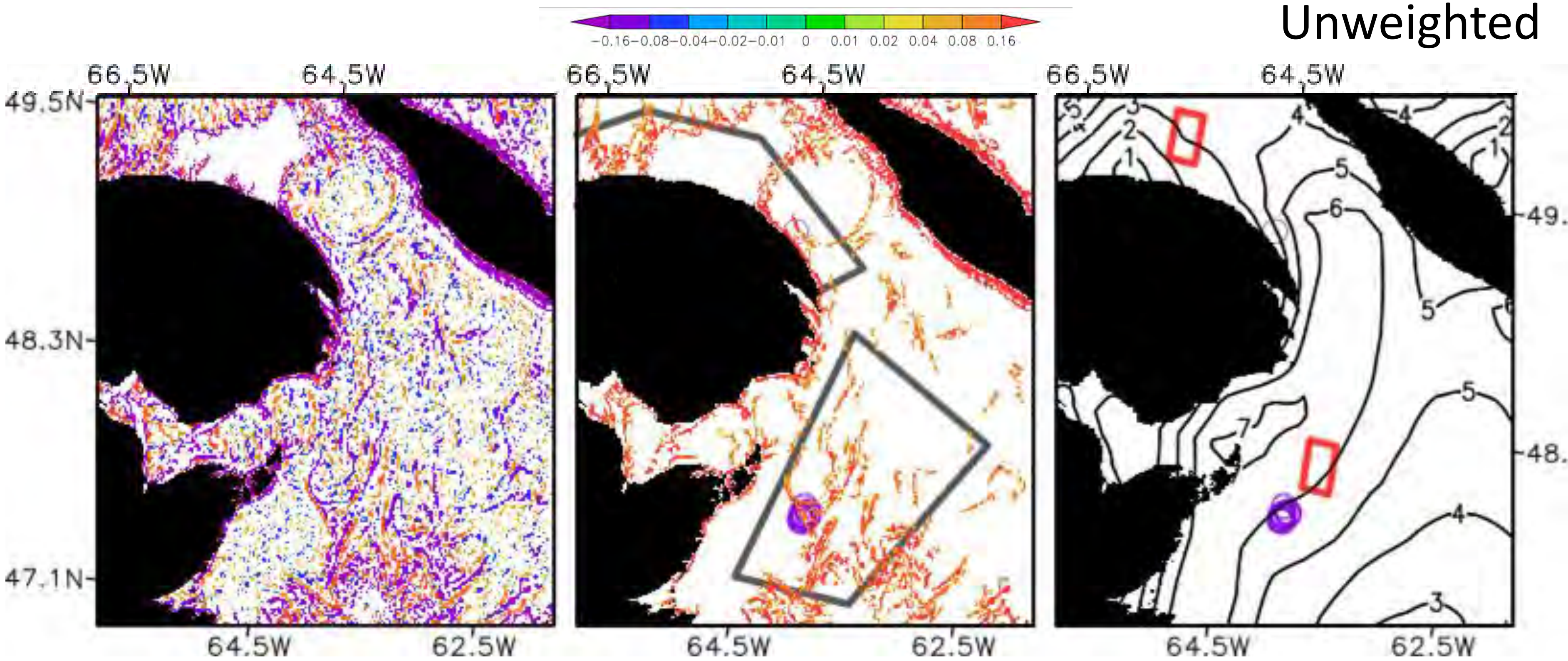

Retaining contrast groups larger than O[10km] also helps to isolate filamentary SAR pattern

Correlation and wind adjustment

- We want to explore SAR filament patterns near right whales but expect SAR contrast to depend nonlinearly on wind speed. Can we identify a *specific* adjustment for Radarsat-2 to emphasize ocean current deformation preferentially?
- Perhaps the simplest nonlinear adjustment is [ERA5 wind speed]^{x} where **x** is determined by maximizing the correlation between SAR contrast (*C*) and ERA5 wind speed (*U*). By design, **association is given by a measurement model that is *nonspecific* about physical process**:
- Linear and nonlinear association (t and ε) and lack of association (ε_C and ε_U) are signal-and-noise terms whose interpretation is based on signal.
- This model can be said to associate measurements with each other, but only by way of what they both measure. Total association is given by $t + \varepsilon$ (in C) and $\alpha_U + \beta_U t + \varepsilon$ (in U), where α_U and β_U are an additive and multiplicative calibration of t in U.

$$
\begin{aligned}
\text{SAR} \quad C &= t + \epsilon + \epsilon_C \\
\text{ERA} \quad U &= \alpha_U + \beta_U t + \epsilon + \epsilon_U \\
Var(C) &= \sigma_t^2 + \sigma_\epsilon^2 + \sigma_C^2 \\
Var(U) &= \beta_U^2 \sigma_t^2 + \sigma_\epsilon^2 + \sigma_U^2 \\
Cov(C,U) &= \beta_U \sigma_t^2 + \sigma_\epsilon^2
\end{aligned}
$$

Correlation and wind adjustment

- A novel decomposition of Pearson correlation $\rho = Cov(C,U)/\sqrt{Var(C)Var(U)}$ is permitted by the linear ($\beta_U \sigma_t^2$) and nonlinear (σ_ε^2) components of $Cov(C,U)$
- **Distance correlation** is a novel measure of nonlinear and nonmonotonic dependence (Székely et al. 2007, Székely and Rizzo 2009) that is comparable to Pearson correlation (Edelmann et al. 2021). For example (en.wikipedia.org/wiki/Distance_correlation)

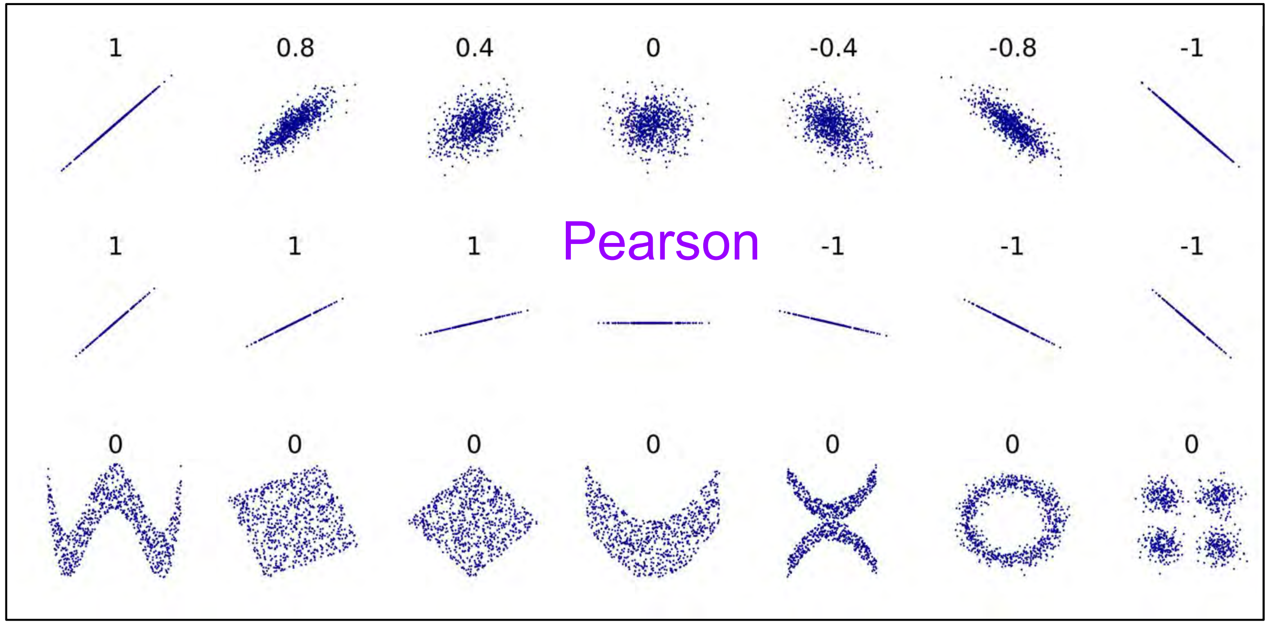

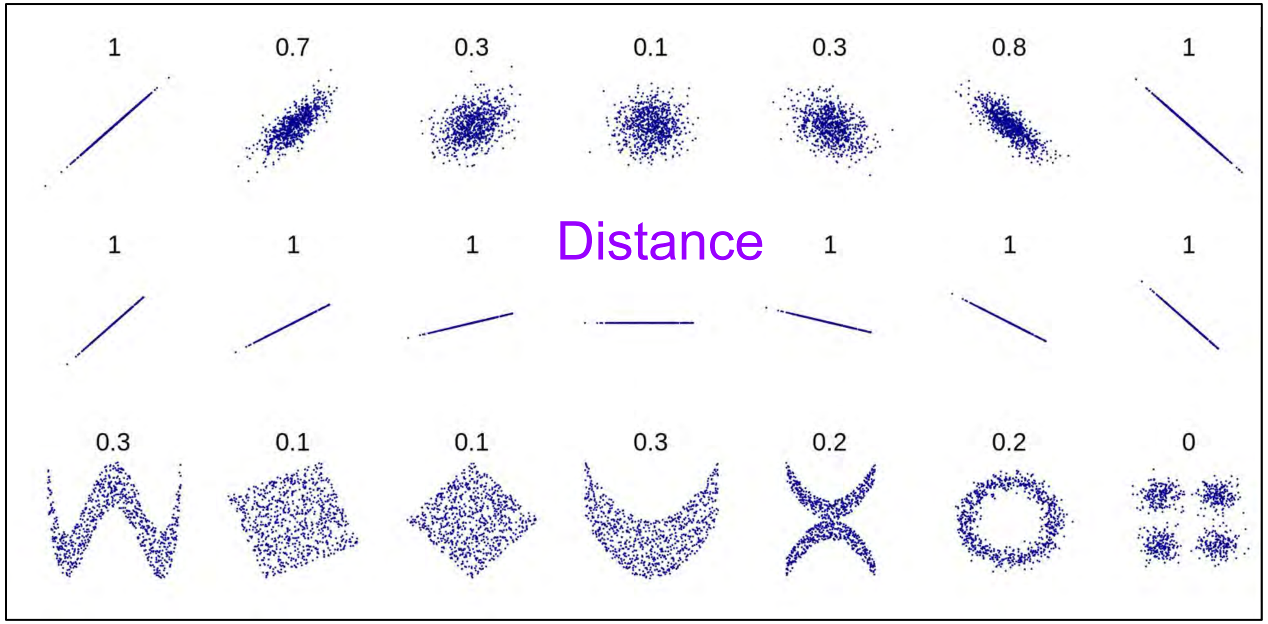

Székely, G. J., and M. L. Rizzo, 2009: Brownian distance covariance. Annals of Applied Statistics, 3, 1236–1265, doi:10.1214/09AOAS312.

Székely, G. J., M. L. Rizzo, and N. K. Bakirov, 2007: Measuring and testing dependence by correlation of distances. Annals of Statistics, 35, 2769–2794, doi:10.1214/009053607000000505.

Edelmann, D., T. F. Móri, and G. J. Székely, 2021: On relationships between the Pearson and the distance correlation coefficients. Stat. Prob. Lett., 169, 1–6, doi:10.1016/j.spl.2020.108960.

Correlation and wind adjustment

- Mid-May to mid-August is when winds are lighter and whale prey near the surface may be more dense
- Wind dependence is more apparent in the seasonal averages (c,d). Wind tends to be stronger and contrast magnitude weaker in the Shediac domain
- Both Pearson correlation (negative) and distance correlation (always positive) are consistent with predictions of an inverse filament contrast dependence on wind speed

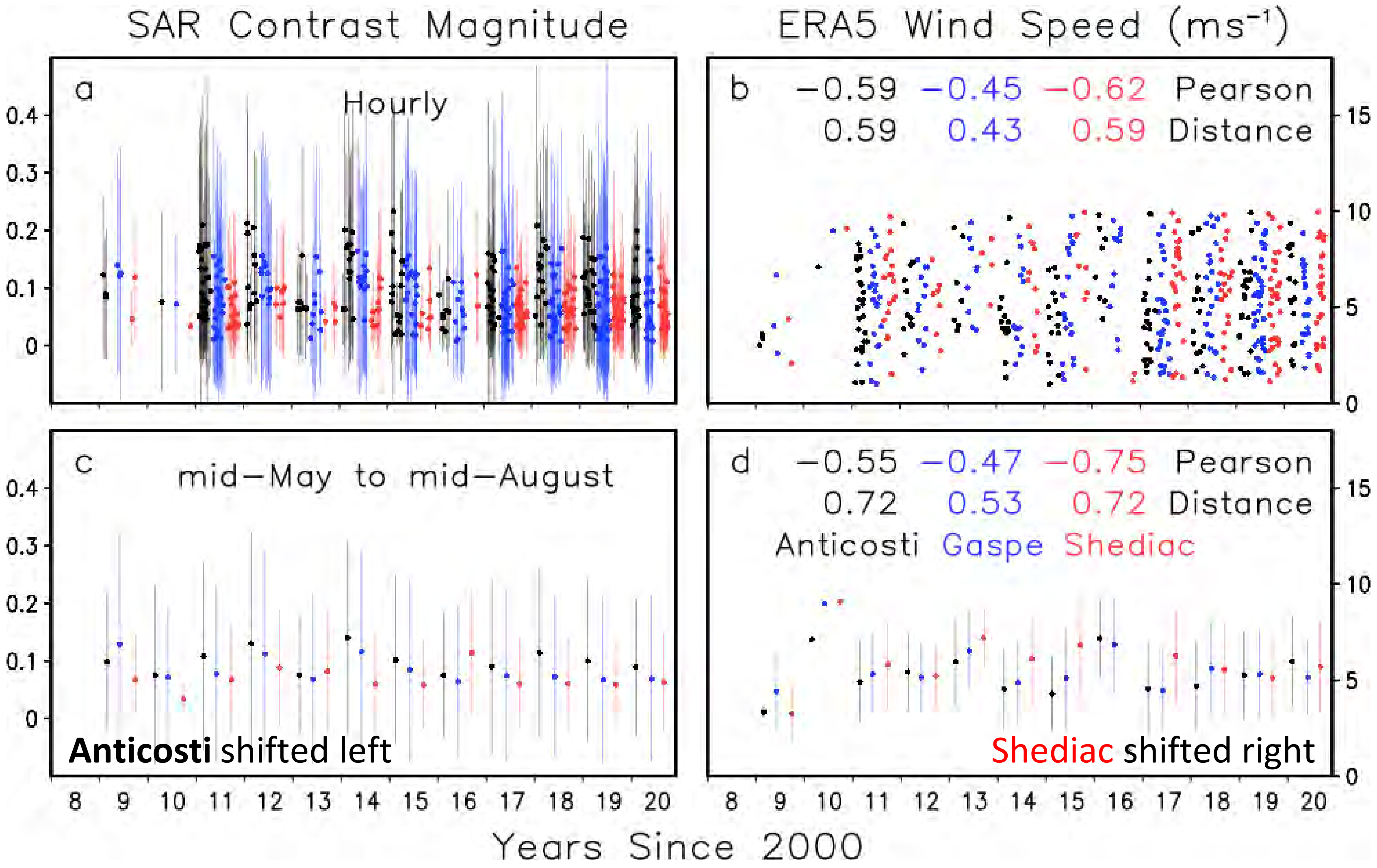

Correlation and wind adjustment

- Peak dependence of Radarsat-2 SAR contrast on ERA5 wind speed (U^x) is given by filled circles for distance correlation (blue) and Pearson correlation (black) magnitude.
- Linear (solid lines) and nonlinear (dashed lines) components of Pearson correlation are obtained using lagged ERA5 samples at 1/2/5-h intervals (see Summary slide). **At negative exponents, Pearson and distance correlation differ more, while Pearson becomes more nonlinear.**
- The vertical line at x = 0.8 is a proposed adjustment that is close to the correlation peaks in all three domains.

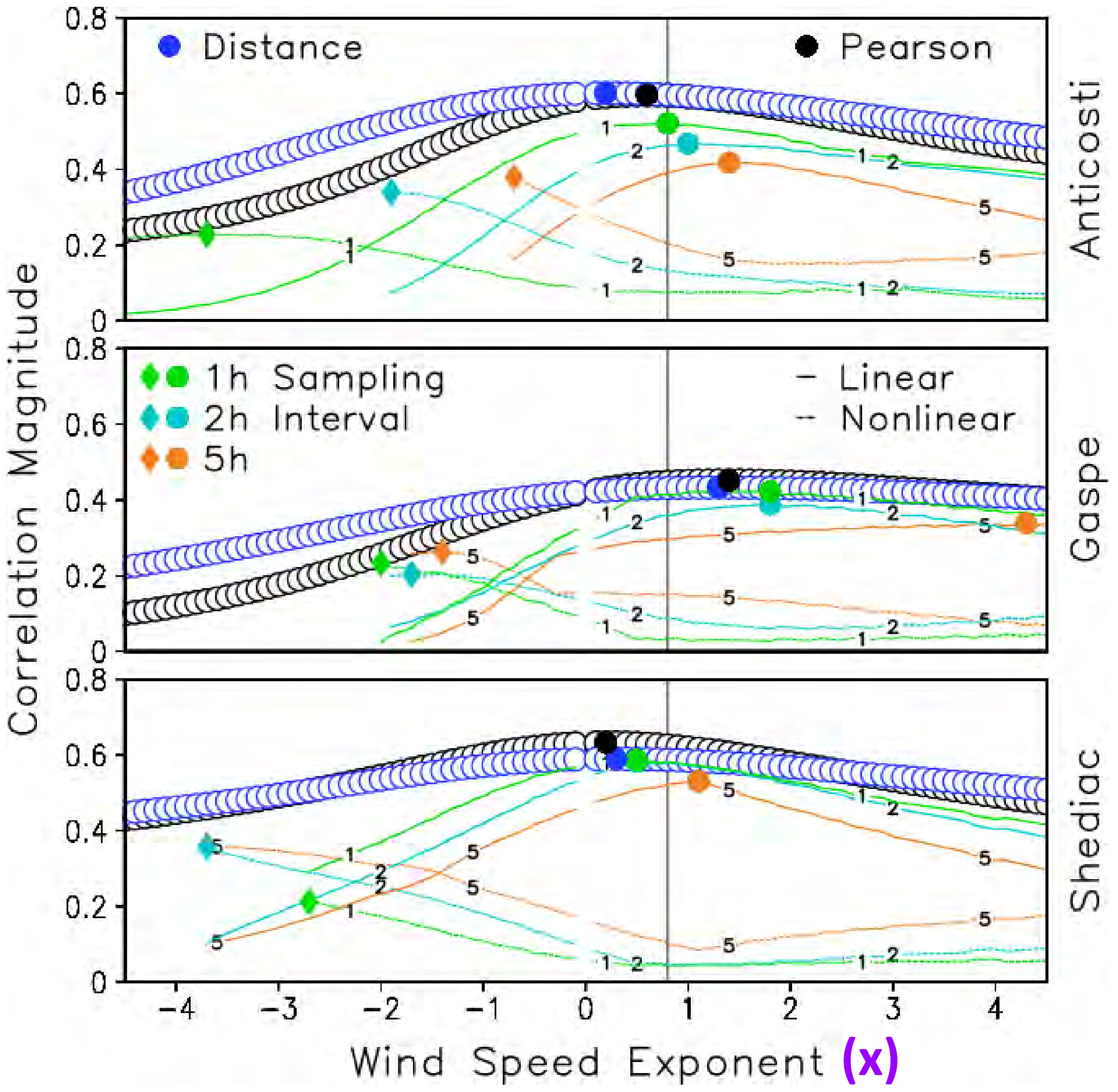

Correlation and wind adjustment

- We opt to scale SAR contrast by $(U/6)^{0.8}$ (i.e., correlation is invariant to a 6-ms^{-1} scaling)
- This yields a reduction in SAR contrast magnitude (a,c). Pearson and distance correlation are reduced to values of less than 0.2 (b).

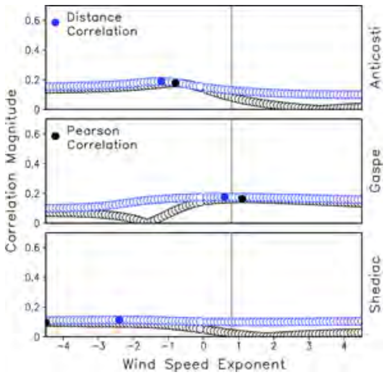

x = 0.8

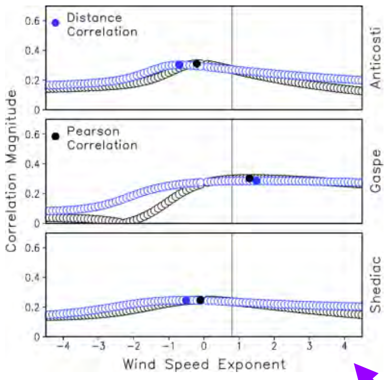

x = 1.0

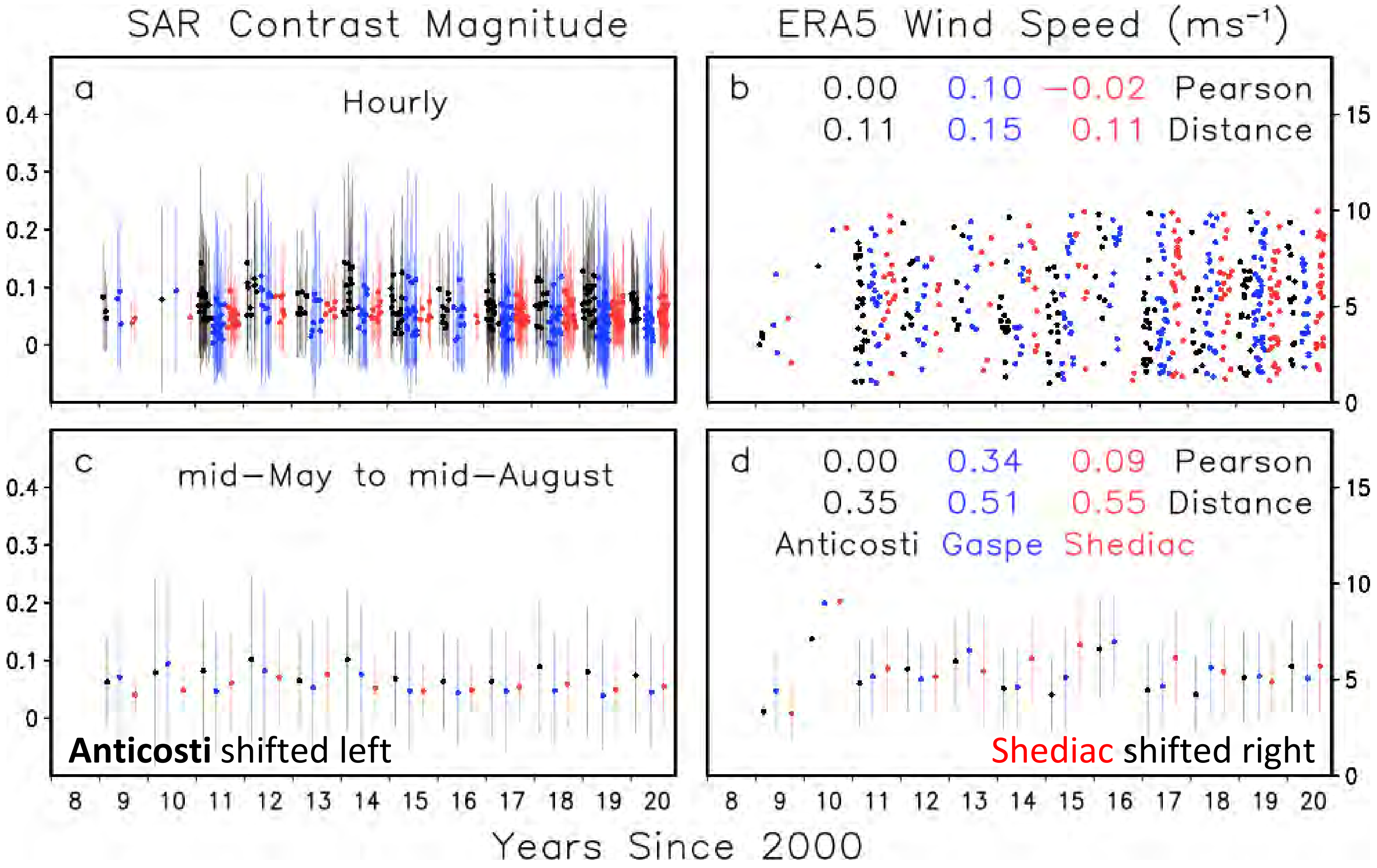

- An exponent of 1.0 does not yield the same degree of correlation reduction

Definition of coherent filaments

Smooth σ_O to 100, 200, 400, 800, 1600, 3200, 6400, and 12800-m resolution

Average contrast of the same sign (σ_O at 800m and $\overline{\sigma_O}$ at 1600/3200/6400m)

Weight contrast by ERA5 wind speed to reduce SAR-wind association

Group adjacent contrasts (small groups < O[10km] are set to zero)

Average contrast magnitude in *fixed* domains (Anticosti, Gaspé, and Shediac)

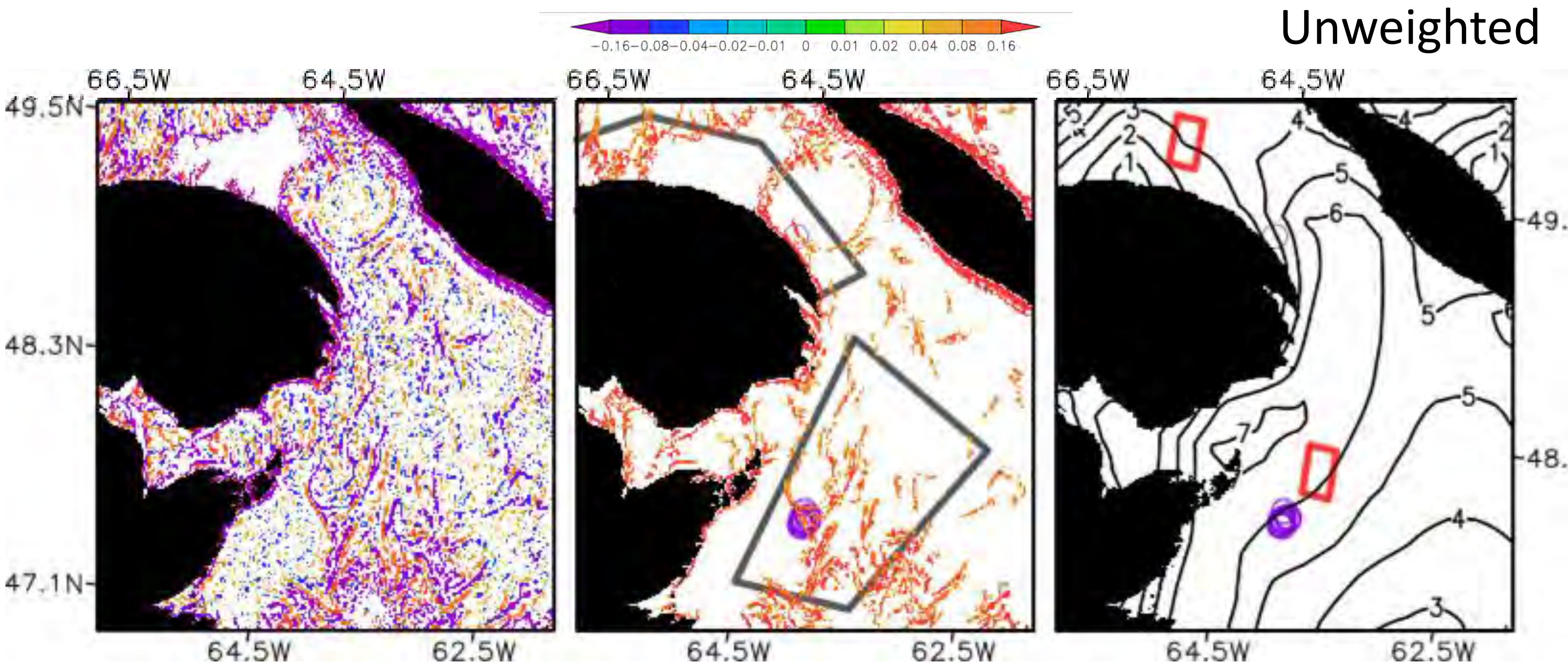

Returning to our example scene:

- Between the Gaspé Peninsula and Anticosti Island is the signature of an anticyclonic eddy (also seen in an Altika pass)
- Extending southward is a surface current that appears to terminate where 21 whales are sighted on this day.

Definition of coherent filaments

Smooth σ_O to 100, 200, 400, 800, 1600, 3200, 6400, and 12800-m resolution

Average contrast of the same sign (σ_O at 800m and $\overline{\sigma_O}$ at 1600/3200/6400m)

Weight contrast by ERA5 wind speed to reduce SAR-wind association

Group adjacent contrasts (small groups < O[10km] are set to zero)

Average contrast magnitude in *fixed* domains (Anticosti, Gaspé, and Shediac)

Weighted

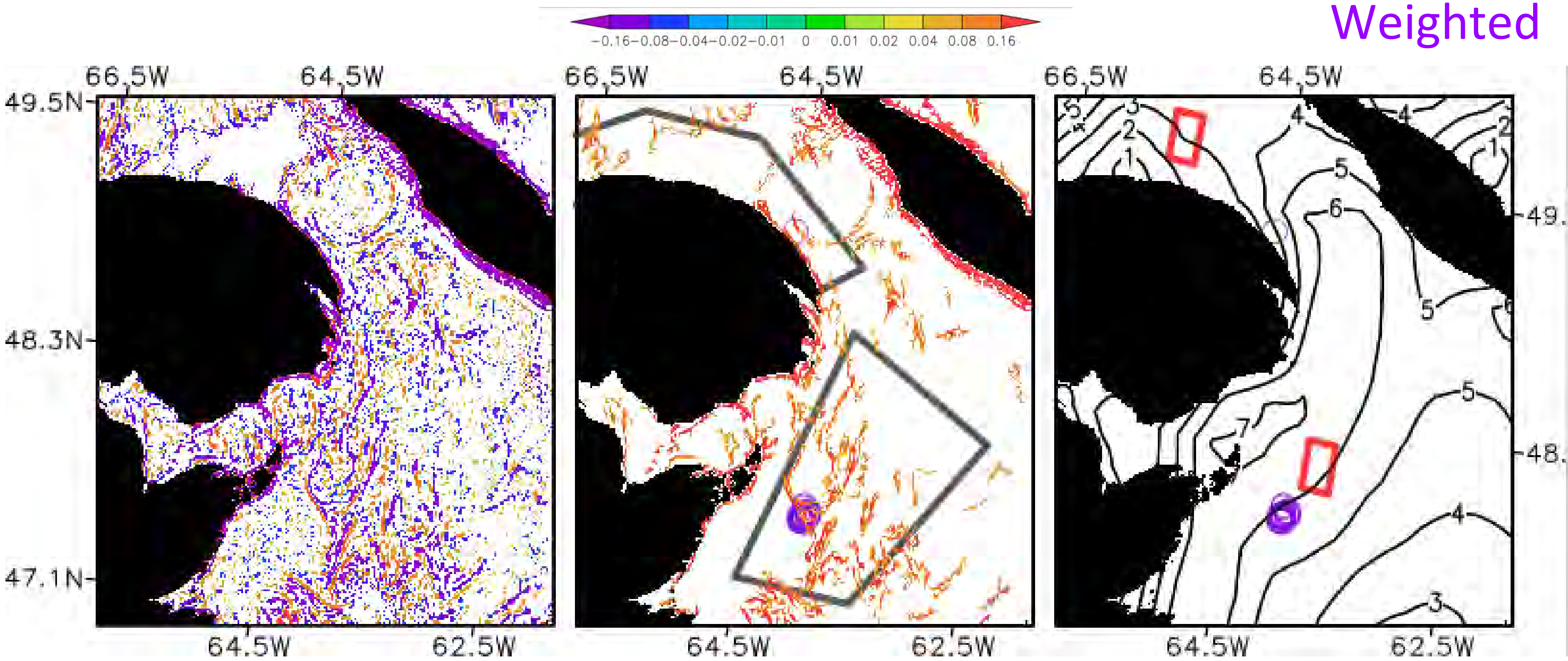

Returning to our example scene:

- Weighted watermass boundaries are largely unchanged, but the orientation of the filaments that mark the boundaries of the southward flowing current seem easier to identify.

Summary of modeling considerations

- When exploring right whale prey aggregation via ocean surface roughness, radar models and observations motivate a reduction in wind dependence. Whales are more often sighted in the Shediac Valley, where winds are *stronger* and SAR contrast is *weaker.*
- Even though ERA5 doesn't assimilate SAR data, we consider error correlation to be part of total (nonlinear) association. Our proposed adjustment ($U^{0.8}$) is mostly linear, and reduces scene-by-scene wind dependence from about 0.6 to 0.2. Pearson and distance correlation indicate that association becomes more nonlinear at negative exponents.
- Regarding complementary modeling, as radar models evolve, is it of interest for measurement models that are *nonspecific* about physical process to guide this evolution? And vice versa, a measure of friction velocity may provide a relevant and interesting dependence here.

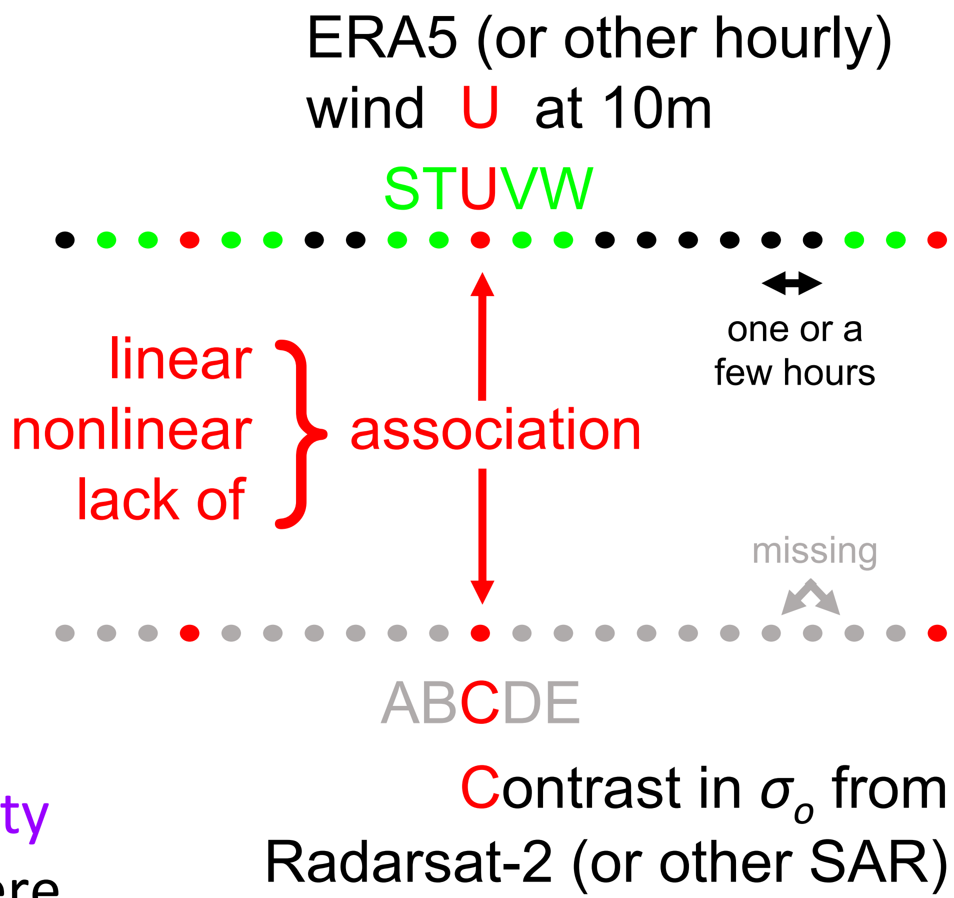

Idealized data and model solutions are at https://github.com/JuliaAtmosOceanHydro/MeasurementModelDemos

Specific measurements in the Gulf of St. Lawrence

Year	Right Whale Sightings	SAR Scenes	Scenes with Whales		Sightings in Scenes	
2015	114/343	86	2	(2%)	2/3	(2%/1%)
2016	100/159	53	3	(6%)	6/9	(6%/6%)
2017	1151/2118	83	11	(13%)	165/278	(14%/13%)
2018	1622/2913	105	4	(4%)	31/33	(2%/1%)
2019	1904/2049	188	31	(16%)	669/705	(35%/34%)
2020	9/9	68	0	(0%)	0/0	(0%/0%)

Table 1: Number of Gulf of St. Lawrence right whale sightings (by group/individual), and SAR scenes per year between 2015 and 2020 (the 2019 and 2020 sightings are preliminary). Included are the number of scenes with right whales, and the number of right whale sightings (by group/individual) collocated with those scenes, with fractions of their total in brackets. A sighting is considered to be temporally collocated with a SAR scene if both occur on the same day. Coverage by SAR (of dashed circle in Fig. 1) is from May to December and includes 11 (2008), 24 (2009), 31 (2010), 99 (2011), 63 (2012), 68 (2013), and 62 (2014) scenes prior to 2015.

WARNING: Information about right whale presence and absence is generally sparse, but opportunistic sightings are more frequent closer to shore and during the summer months. Sighting effort also depends on observing conditions (e.g., visibility depends on sea state, fog, precipitation, and time of day). Effort increased after 2016 but was affected by COVID-19; no effort corrections are employed here.